J. Biochem. 125, 1151-1159 (1999)

Solution Structure of the SH2 Domain of Grb2/Ash Complexed with EGF Receptor-Derived Phosphotyrosine-Containing Peptide[1]

Shigeo Tsuchiya,*,† Kenji Ogura,*,‖ Hideki Hatanaka,* Koji Nagata,* Hiroaki Terasawa,*,‖ Valsan Mandiyan,‡ Joseph Schlessinger,‡ Saburo Aimoto,§ Hiromichi Ohta,† and Fuyuhiko Inagaki*,‖,2

*Department of Molecular Physiology, Tokyo Metropolitan Institute of Medical Science, 3-18-22 Honkomagome, Bunkyo-ku, Tokyo 113-8613; †Department of Chemistry, Faculty of Science and Technology, Keio University, 3-14-1 Hiyoshi, Kohoku-ku, Yokohama 223; ‡Department of Pharmacology, New York University Medical Center, New York, New York 10016, USA; §Protein Research Institute, Osaka University, 3-2 Yamadaoka, Suita-shi, Osaka 565; and ‖CREST, JST

Received January 7, 1999; accepted March 20, 1999

^{1}H, ^{13}C, and ^{15}N NMR resonances of the SH2 domain of Grb2/Ash in both the free form and the form complexed with a phosphotyrosine-containing peptide derived from the EGF receptor were assigned by analysis of multi-dimensional, double- and triple-resonance NMR experiments. From the chemical shift changes of individual residues upon peptide binding, the binding site for the peptide was mapped on the structure of Grb2/Ash SH2. The peptide was not recognized by the groove formed by the BG and EF loops, suggesting that the EGFR peptide does not bind to Grb2/Ash SH2 in an extended conformation. This was supported by analysis of the binding affinity of mutants where residues on the BG and EF loops were changed to alanine. The present results are consistent with the recently reported structures of Grb2/Ash SH2 complexed with BCR-Abl and Shc-derived phosphotyrosine containing peptides, where the peptide forms a turn conformation. This shows that the specific conformation of the phosphotyrosine-containing sequence is required for the SH2 binding responsible for downstream signaling.

Key words: EGF receptor, Grb2/Ash, NMR, SH2 domain, solution structure.

Growth factor receptor bound protein 2 or abundant Src homology (Grb2/Ash) (*1*) is an adaptor protein with a domain structure SH3-SH2-SH3. The two SH3 domains of Grb2/Ash bind to proline-rich sequences in the carboxyl terminal region of the guanine nucleotide exchange factor, Son of sevenless (Sos) in the cytosol (*2-4*). Upon EGF stimulation, Grb2/Ash SH2 binds to the EGF receptor directly or indirectly through proteins such as Shc, FAK, Syp, and IRS-1, by recognizing phosphotyrosine-containing sequences and relocating Sos to the plasma membrane to allow interation with Ras (*5, 6*). Thus Grb2/Ash mediates signal transduction from a variety of extracellular stimuli to Ras. The consensus phosphotyrosine-containing sequence for Grb2/Ash SH2 binding has been studied extensively by phosphopeptide inhibition and peptide library screening (*7*) and is now accepted to be pTyr-(Ile/Leu/Val/Met)-Asn-(Val/Pro/Gln), where the Asn at pTyr+2 is essential, implying that Grb2/Ash SH2 recognizes phosphotyrosine-containing sequences in a specific manner.

Recently, the solution structure of free Grb2/Ash SH2 was reported by NMR (*8*). The phosphotyrosine-binding pocket of Grb2/Ash SH2 is similar to that of other SH2 domains; however, the side chain of Trp121 (EF1) in Grb2/Ash occupies the corresponding pTyr+3 binding pocket in Src SH2 so that phosphotyrosine-containing peptide does not seem to bind in an extended conformation similar to other SH2 domains. The X-ray crystal structure of Grb2/Ash SH2 complexed with a BCR-Abl-derived peptide (Lys-Pro-Phe-pTyr-Val-Asn-Val) demonstrated that the peptide forms a β-turn at the pTyr, pTyr+1, pTyr+2, and pTyr+3 positions (*9*). These studies prompted us to investigate the three dimensional structure of the Grb2/Ash SH2 domain complexed with an EGF receptor-derived peptide (Glu-pTyr-Ile-Asn-Gln-Ser-Val, hereafter referred to as the EGFR-peptide). The EGF receptor is a physiologically relevant target protein for Grb2/Ash SH2, and the signal transduction pathway mediated by the Grb2/Ash-EGF receptor complex forms part of a major mitogenic signaling pathway (*2-4*). Therefore, elucidation of the structural basis for the molecular recognition between Grb2/Ash and the EGFR-peptide is of significant interest. In the present study, we assigned ^{1}H, ^{13}C, and ^{15}N resonances of the free and complexed forms of Grb2/Ash SH2 with the EGFR-peptide. On the basis of the chemical shift perturbation between the free and EGFR-peptide bound forms of Grb2/Ash SH2, along with mutational studies, we discuss the binding mode of the EGFR-peptide.

[1] This work was supported in part by grants from the Ministry of Education, Science, Sports and Culture of Japan, and from CREST of Japan Science and Technology.

[2] To whom correspondence should be addressed at: Department of Molecular Physiology, Tokyo Metropolitan Institute of Medical Science, 3-18-22 Honkomagome, Bunkyo-ku, Tokyo 113-8613. Fax: +81-3-3823-1247, E-mail: inagaki@rinshoken.or.jp

MATERIALS AND METHODS

Expression and Purification of the Grb2/Ash SH2 Domain and Its Mutants—The plasmid in which the Grb2/Ash SH2 domain (residues His58 to Thr159 with an additional two N-terminal residues, Gly-Ser) was expressed was constructed using a pGEX-4T-2 vector. For preparation of $^{13}C/^{15}N$ labeled Grb2/Ash SH2, transformed *Escherichia coli* BL21 (DE3) cells were grown in M9 minimal medium containing $^{15}NH_4Cl$ (1 g/liter), [*ul*^{13}C]-glucose (2 g/liter), and CELTONE-CN (Martek, USA) (1 g/liter) at 37°C and induced at $OD_{600}=1.0$ with 0.4 mM isopropyl-thio-β-D-galactoside. The cells were collected after 4 h, suspended in 20 mM potassium phosphate buffer, pH 7.4, containing 5 mM DTT, 1 mM PMSF, and 1 mM EDTA, and then sonicated and centrifuged. The supernatants were incubated with glutathione Sepharose 4B beads (Pharmacia, Sweden) for 1 h at 4°C. After extensive washing in potassium phosphate buffer, the GST fusion proteins were eluted with 20 mM reduced glutathione, 50 mM Tris-HCl, and 2 mM DTT, pH 8.2, and fractions were collected. The proteins were cleaved with trypsin (0.01%, w/w, fusion protein) for 1 h at 23°C. The buffer was changed to 20 mM HEPES, 2 mM DTT, pH 7.5, using a desalting column. The protein was applied to a Mono S 10/10 HPLC column (Pharmacia, Sweden) and eluted with a 0–600 mM NaCl gradient in 20 mM HEPES, pH 7.5. Finally, the SH2 domain was purified on a Superose 12 column (Pharmacia, Sweden) eluted with 20 mM potassium phosphate buffer and 150 mM NaCl, pH 6.3.

The codons for Leu 120 (βE4), Ser 141 (BG3), Arg 142 (BG4), and Asn 143 (BG5) were changed to encode Ala. The mutants were subcloned into the pGEX-4T-2 GST bacterial expression vector. The subcloned vectors were transformed into *Escherichia coli* JM109 and sequenced.

Peptide Synthesis—A phosphotyrosine-containing peptide (Glu-pTyr-Ile-Asn-Gln-Ser-Val) corresponding to the sequence of EGFR (1067-1073) was synthesized by solid-phase Fmoc strategy using Na-Fmoc-*O*-(*O,O*-dimethoxyphosphoryl)-L-tyrosine [Fmoc-Tyr(OP(OMe)$_2$)] (Watanabe Chem., Japan). The synthesized peptide was purified by reverse-phase HPLC on a Resource RPC column (Pharmacia, Sweden). The purified peptide was characterized by mass spectroscopy and amino acid analysis.

NMR Sample Preparation—Protein samples for NMR experiments were prepared in buffers containing 20 mM potassium phosphate and 150 mM NaCl at pH 6.3. Buffer exchange and sample concentration were performed with a 10 kDa cutoff Centricon concentrator (Amicon, USA) at 4°C. The final protein concentration was 1.5 mM in a sample volume of 230 μl. Approximately 1.5 mol equiv. of the phosphotyrosine-containing peptide were added to the sample solution. After a final concentration step with the 10 kDa cutoff concentrator, the samples were adjusted to 10% ^2H_2O or exchanged into a sample buffer system prepared with 99% ^2H_2O and adjusted to 5 mM DTT-d_{10} and 0.5% (w/v) NaN_3 from a freshly concentrated stock solution. All samples were placed in restricted volume 5 mm NMR tubes (Shigemi, Japan).

NMR Spectroscopy—All NMR spectra were recorded at a sample temperature of 28°C on Varian Unity-plus 600 and Unity 500 spectrometers equipped with an Ultra Shim unit (Resonance Research, USA), three rf channels, and a pulsed field gradient triple-resonance probe with an actively shielded *z* gradient coil. Proton chemical shifts were referenced to internal DSS (0 ppm). ^{13}C and ^{15}N chemical shifts were referenced indirectly to liquid NH_3 and DSS according to Bax and Subramanian (*13*). States-TPPI (*14*) quadrature detection was employed in the indirect dimensions. All heteronuclear experiments and isotope-filtered experiments were adapted to incorporate *z*-gradient pulses to suppress artifacts and eliminate the water resonance. Pulsed field gradients were also used for coherence selection in experiments to detect NH protons. The 2D homonuclear-correlated spectra were processed with the standard VNMR (Varian Instruments, USA) software, while other spectra were processed by the NMR Pipe program (*15*) on a Sun Ultra-1 workstation. Time domain convolution was used to remove the solvent signal (*14*), and the indirect ^{15}N and/or ^{13}C dimensions were extended as needed with linear prediction. Multidimensional data peak picking was employed using home-written software (Hatanaka, unpublished). NMR data visualization and analysis were performed with the Felix 95.0 program (Molecular Simulations, USA) and home-written software (*16*) on a Sun SPARC Station computer.

Chemical Shift Assignment—The backbone resonance assignments of the Grb2/Ash SH2 domain were obtained by a sequential walk in the following triple resonance spectra using a 1.5 mM solution of uniformly $^{13}C/^{15}N$-labeled protein complexed with 1.5 mol equiv. of EGFR-peptide in H_2O solution. All of the following spectra were collected on a Unity 500 spectrometer with a ^1H (F_3) carrier frequency at 4.75 ppm with a spectral width of 7,000 Hz and a ^{15}N (F_2) carrier frequency at 117.7 ppm with a spectral width of 1,800 Hz.

To assign the protein-backbone resonances, the following four 3D experiments were carried out. HNCA and HN(CO)CA experiments (*17*) were performed with a ^{13}C (F_1) carrier frequency at 55.3 ppm, a spectral width of 3,600 Hz, and eight transients for each increment. CBCANH and CBCA(CO)NH experiments (*17*) were collected with a ^{13}C (F_1) carrier frequency at 41.0 ppm, a spectral width of 8,800 Hz, and 16 transients for each increment. The walk for sequential assignments started at several spin systems assigned to specific amino acid types based on the characteristic $^{13}C^{\alpha}/^{13}C^{\beta}$ chemical shifts. The peptide fragments connected by the walk were unambiguously assigned to specific sequences on Grb2/Ash SH2 considering the alignments of the amino acid types.

Other resonances of the Grb2/Ash SH2 domain were subsequently assignal by the following five experiments. The 3D C(CO)NH (*18*) experiment was performed with a ^{13}C (F_1) carrier frequency at 41.0 ppm, a ^{13}C spectral width of 8,800 Hz, and 32 transients for each increment in 90% H_2O solution. The 3D HBHA(CO)NH (*18*) experiment was performed with ^1H (F_1) spectral width of 3,500 Hz, and 16 transients for each increment in 90% H_2O solution. 3D HNCO (*17*) was collected with a ^{13}C (F_1) spectral width of 1,800 Hz centered on 177 ppm, and eight transients. 3D HN(CA)HA (*19, 20*) was collected with 16 transients, and a ^1H (F_1) spectral width of 2,000 Hz. The assignments of the aromatic resonances of the Grb2/Ash SH2 domain were achieved with the conventional 2D COSY, TOCSY, and NOESY spectra using ^{15}N-labeled sample in 90%

H_2O solution.

Fluorescence Measurements—Fluorescence measurements were made with a Shimazu RF-5000 fluorescence spectrometer (Shimazu, Kyoto). Aliquots of EGFR-peptide at 500 μM were added successively to the 2.5 μM Grb2/Ash SH2 solution. The excitation wavelength was 295 nm with a band width of 5 nm; emission was observed with band width of 10 nm.

RESULTS AND DISCUSSION

Assignments of NMR Resonance—Figure 1 shows the ^1H-^{15}N HSQC spectrum of Grb2/Ash SH2 complexed with EGFR-peptide at a 1.5 molar ratio. The sequential resonance assignments of Grb2/Ash SH2 complexed with EGFR-peptide were achieved based on the analysis of a suite of HNCA, HN(CO)CA, CBCANH, and CBCA(CO)NH spectra. The walk of resonance assignments from Arg67 to Lys76 is shown in Fig. 2, where the strips of the CACBNH spectra are aligned. In the CBCANH spectrum, cross peaks between NH(i) and both intraresidual Cα(i), Cβ(i), and interresidual Cα($i-1$), Cβ($i-1$) were observed so that the correlation of the cross peaks in each strip link (i)th and ($i-1$)th residues. Thus, most of the main-chain resonances were unambiguously assigned. Aliphatic ^1H and ^{13}C resonances were assigned using HBHA(CO)NH, HN(CA)HA, C(CO)NH, H(CCO)NH, ^1H-^{13}C CT-HSQC, and HCCH-TOCSY spectra.

The spin systems of the aromatic side-chain proton resonances were identified with the conventional two-dimensional DQF-COSY and TOCSY spectra. The ^{15}N-filtered NOESY spectrum on the ^{15}N-labeled protein in 90% H_2O/10% ^2H_2O provided the correlation between aromatic protons and aliphatic protons without overlap of the amide proton resonances, thus correlating the spin systems of aromatic protons with Hβ resonances. 2D isotope-filtered TOCSY and NOESY experiments (*10*) were performed to detect proton resonances of the unlabeled EGFR-peptide in the complex. However, except for the aromatic proton resonances of the phosphotyrosine residue, the resonances were too broad to be detected possibly due to exchange broadening. The ^1H, ^{15}N, and ^{13}C resonance assignments of Grb2/Ash SH2 complexed with the EGFR-peptide are summarized in Table I.

Secondary Structure of Grb2/AshSH2 Complexed with EGFR-Peptide—Once the sequential assignments of the main chain resonances were completed, NOE correlations from 3D ^{15}N-edited NOESY and ^{13}C-edited NOESY spectra were analyzed to obtain the secondary structure of Grb2/Ash SH2. The analyses of the sequential and short-range NOEs are summarized in Fig. 3. The secondary structure was deduced based on the sequential and short range NOE connectivities. The NOE connectivity patterns support the presence of α helices at residues 66-73 and

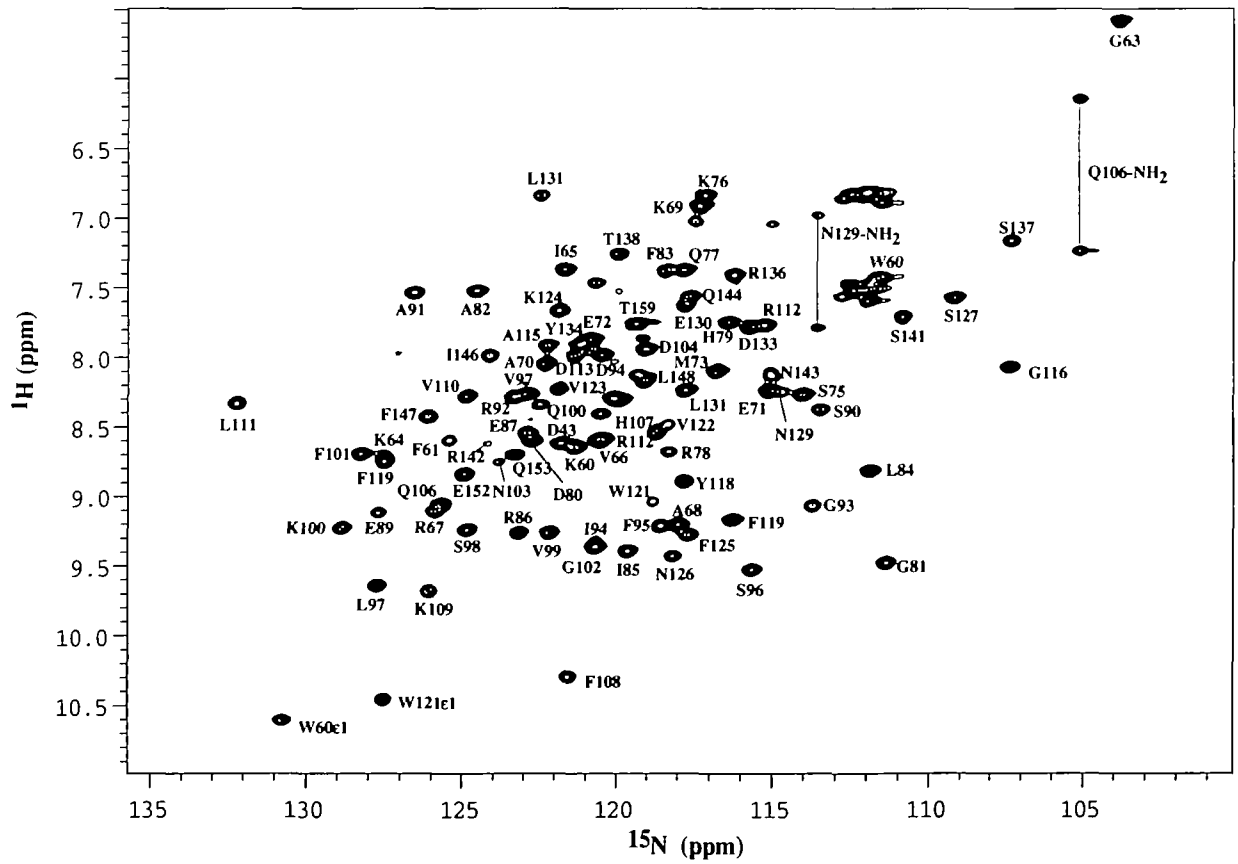

Fig. 1. **Two-dimensional ^1H-^{15}N HSQC spectrum of the ^{15}N-labeled Grb2 SH2 domain complexed with unlabeled EGFR-peptide.** The peaks are labeled with the amino acid residue assignments. Unlabeled peaks are not assigned. Sample solutions with a 2.0 molar ratio of EGFR-peptide/Grb2 SH2 were used for NMR measurements.

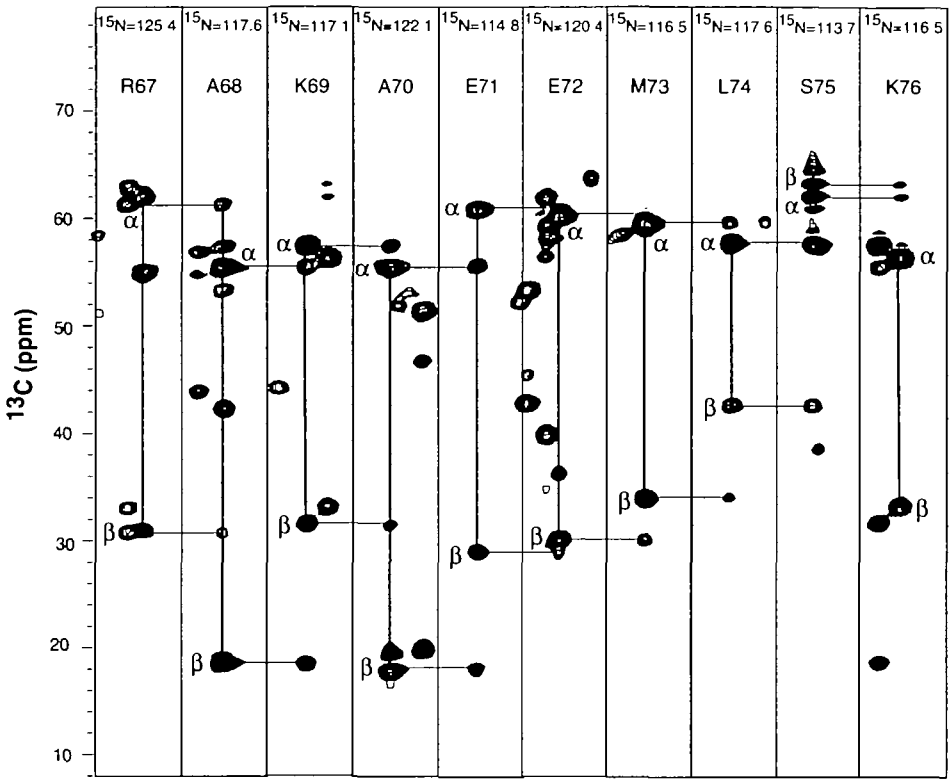

Fig. 2. **Sequential walk of Grb2 SH2 complexed with the EGFR-peptide.** The residues from Arg67 to Lys76 were connected by the sequential walk on the CBCANH spectrum.

TABLE I. ^{1}H, ^{15}N, and ^{13}C resonance assignments (ppm)[a] for the Grb2 SH2 domain complexed with the EGFR-peptide.

Residue	N	NH	Cα	Hα	Cβ	Hβ	Cγ	Hγ	Cδ	Hδ	Cother	Hother
H58												
P59				4.23								
W60	113.5	7.44	54.5	4.87	28.8	3.33, 3.04				6.60		Hε$_1$10.68, Hζ$_3$6.73, Hε$_3$7.46, Hζ$_2$7.94, Hη$_2$6.78
F61	124.8	8.62	57.5	5.32	38.1	2.47, 2.34				7.14		Hε7.43
F62	127.1	8.83	57.1	4.41	40.7	3.31, 2.62				7.26		Hε6.93, Hζ7.36
G63	103.2	5.56	47.0	3.84, 3.60								
K64	127.1	8.81	55.6	4.61	31.0	1.96, 1.73	25.4	1.32		1.45		
I65	121.5	7.37	57.1	4.89		1.86		1.77		1.05		Hγ″1.05
P66				4.51	32.9	2.62, 1.92	28.0	2.11	51.1	4.07		
R67	125.4	9.17	59.4	3.51		1.81, 1.68		1.19, 0.71				
A68	117.6	9.29	54.5	4.20	18.3	1.45						
K69	117.1	6.97	57.7	4.31	31.4	1.99	24.7	1.56	28.0	1.80	Cε42.2	Hε3.03
A70	122.1	8.10	54.5	3.97	18.3	1.52						
E71	114.8	8.32	59.7	4.00	28.4	2.34, 2.13		2.73				
E72	120.4	7.94	59.0	4.01	29.9	2.24	35.8	2.45, 2.17				
L74	117.6	8.31	57.7	3.99	42.2	1.91, 1.17	25.4	1.73	22.8	0.65	Cδ′25.8	Hδ′0.73
S75	113.7	8.33	61.9	4.13	62.3	4.06, 3.99						
K76	116.5	6.89	55.6	4.36	32.9	2.10, 1.82	25.4	1.53	28.8	1.65		
Q77	117.6	7.44	54.5	4.20	28.8	2.33	34.4	2.73				
R78	117.6	8.72	56.3	4.28	31.0	1.70, 1.62	26.3	1.49	42.9	3.17		
H79	116.0	7.85	54.5	4.94	30.6	3.13						Hε$_1$7.87, Hδ$_2$6.87
D80	122.6	8.72	55.6	4.58	41.1	2.88, 2.77						
G81	111.0	9.55	45.2	5.11, 3.26								
A82	126.3	7.62	52.6	5.10	18.7	1.45						
F83	118.7	7.45	54.8	6.16	44.0	3.26, 3.18				7.94		Hε6.67, Hζ7.08
L84	111.5	8.88	54.1	4.68		1.73	27.6	0.37	25.8	0.73, 0.73		
I85	119.3	9.45	59.3	5.52	39.2	2.33		1.92, 1.44	12.7	0.77	Cγ″18.3	Hγ″1.28
R86	122.6	9.33	51.9	5.32	33.6	2.21, 1.36		2.47, 1.77				
E87	122.6	8.63	54.9	4.61		2.01, 1.87		2.48, 2.22				
S88	120.4	8.67	57.8	4.27	62.3	3.93, 3.74						
E89	127.6	9.16	57.8	4.18		2.24, 2.14	36.6	2.18, 2.43				
S90	113.2	8.42	59.3	4.33	64.2	3.96, 3.86						

TABLE I. Continued

Residue	N	NH	Cα	Hα	Cβ	Hβ	Cγ	Hγ	Cδ	Hδ	Cother	Hother
A91	125.9	7.61	48.9	4.75		1.22						
P92			63.4	4.38	31.4	2.29, 1.82	28.0	2.10, 1.95	50.0	3.57, 3.47		
G93	113.2	9.15	44.8	4.24, 3.46								
D94	119.8	8.05	52.2	4.89	42.6	2.84, 2.91						
F95	118.2	9.32	57.7	5.54	41.8	2.84, 3.23				7.37		Hε7.57, Hζ7.72
S96	115.4	9.59	57.7	5.38	65.3	3.59, 4.12						
L97	127.6	9.71	53.3	5.41	45.5	1.24, 1.84	28.4	1.64	26.1	0.73, 0.46		
S98	124.3	9.32	57.8	5.54	65.7	2.84, 3.23						
V99	122.1	9.34	58.9	5.27	36.2	1.91	20.6	0.93, 0.93			Cγ′22.8	
K100	128.7	9.30	56.0	4.57	35.1	1.77, 2.13	25.8	1.55, 1.75	29.5	1.75	Cε42.9	Hε3.08
F101	128.2	8.75	58.6	4.68	41.1	2.83, 2.88				7.14		Hε7.33, Hζ7.72
G102	120.4	9.44	46.3	3.55, 3.70								
N103	123.7	8.84	52.6	4.85	38.5	2.69, 3.01						
D104	118.7	8.00	52.6	5.03	44.8	2.79						
V105	119.8	8.37	60.8	4.55	34.0	1.79	22.4	0.45, 0.91				
Q106	125.4	9.12	55.2	4.36		1.77, 1.95		2.29				
H107	118.2	8.64	54.1	5.92	34.0	2.76, 2.87						Hε$_1$ 6.78
F108	120.9	10.37	55.6	4.80		2.64, 3.00				6.93		Hε7.36, Hζ7.25
K109	125.4	9.77	54.5	4.13	31.4	0.80, 1.30	23.2	0.71, 0.79	26.3	1.30	Cε39.9	
V110	124.3	8.33		3.96	29.5	2.38	20.6	0.73, 1.05			Cγ′23.5	
L111	132.1	8.42	53.7	4.14	41.1	0.58, −0.07	26.5	1.23	23.5	0.59		
R112	114.8	7.84	51.9	5.67	32.5	1.58, 1.78	26.5	1.33		3.03		
D113	120.9	7.99	51.5	5.07	42.2	3.31, 2.50						
G114		8.64	46.3	3.91								
A115	122.1	7.96	51.1	4.59	19.8	1.48						
G116	107.1	8.13	45.2	3.65, 4.23								
K117	120.9	8.73	56.0	4.56	32.1	1.84, 2.03	26.1		28.4	1.55	Cε42.6	Hε2.95
Y118	117.6	8.98	56.3	5.63	41.4	2.64, 2.78				6.96		Hε6.89
F119	116.0	9.22	57.1	5.14	41.4	2.81, 3.48				7.25		Hε6.78, Hζ6.16
L120	116.0	9.33		4.55	45.5	0.93, 1.91	26.1	1.49	25.8	0.46	Cδ′24.3	Hδ′0.66
W121	118.2	9.14	56.3	5.30	31.0	3.54, 3.61				7.51		Hε$_1$10.53, Hζ$_3$7.34, Hε$_3$7.94
V122	117.6	8.57	63.4	4.21	34.7	2.13	21.3	0.95, 1.02				
V123	121.5	8.32	63.4	3.59	31.7	1.74	22.0	0.33, 0.99				
K124	121.5	7.76	53.7	4.80	35.5	1.42, 1.59	25.4	0.87, 1.28	28.8	1.20	Cε41.1	Hε1.76, Hε′2.30
F125	117.1	9.33	56.0	4.93	43.3	2.81, 3.43				7.26		Hε6.93, Hζ6.16
N126	117.6	9.51	54.5	4.92	39.2	3.03, 3.13						
S127	108.7	7.62	56.0	4.75		4.07, 4.18						
L128	118.6	8.65	56.3	3.60	41.8	1.22, 1.54	26.5	1.09	24.7	0.32	Cδ′23.5	Hδ′0.43
N129	114.9	8.35	56.3	4.29	38.1	2.82, 2.88						
E130	117.6	7.70		3.95		2.19	37.3	2.38, 2.46				
L131	121.1	6.73	58.8	2.15	42.2	1.18, 1.72	27.6	1.41	24.0	0.53	Cδ′28.0	Hδ′0.87
V132	117.5	7.82	66.0	2.78	31.4	1.47	21.3	0.15, −0.25			Cγ′22.8	
D133	115.4	7.86	57.1	4.20	39.9	2.63						
Y134	121.0	7.96	60.8	4.11	39.6	2.63, 3.04				6.34		Hε6.74
H135		7.61	57.5	5.28	26.3	2.70, 3.42						
R136	116.0	7.47	57.5	4.63	30.3	1.72, 1.78	26.3			3.62		
S137	107.1	7.22	57.5	4.30	64.2	3.86, 3.82						
T138	119.3	7.31	62.7	4.47	69.8	3.02	21.3	1.30				
S139		7.16	57.7	4.20	63.1	3.61, 3.99						
V140	119.3	8.37	62.3	3.79	31.7	1.33	20.6	0.32, 0.32				
S141	110.4	7.77	54.5	5.02	64.2	3.62, 3.79						
R142	123.7	8.73	57.7	4.07	30.3	1.29, 1.57	26.9	0.76, 0.99	42.9	2.46		
N143	114.8	8.16	53.0	4.70	39.9	2.70, 2.80						
Q144	117.1	7.63	53.4	4.48	32.1	1.51, 1.65		2.01, 2.22				
Q145		8.71	54.5	4.01	28.4	1.94, 2.03	33.6	2.24				
I146	123.7	8.06	60.1	3.91	39.9	1.30		0.56, −0.03	12.5	0.26	Cγ′17.6	Hγ″0.56
F147	125.9	8.52	54.1	4.95	40.3	2.68, 3.13				6.87		Hε7.16
L148	118.7	8.25	54.9	4.43	39.2	0.47, 0.93	25.8	1.38	25.4	−0.08	Cδ′21.7	Hδ′0.31
R149	123.2	8.35	53.4	4.67	34.0	1.73, 1.91	26.9	1.76	43.7	3.28		
D150	121.8	8.70	54.9	4.90	40.7	2.62, 2.88						
I151	120.4	9.41	62.7	3.90		1.88	28.8	1.06, 1.73	14.0	0.77	Cγ$_2$17.6	Hγ$_2$0.96
E152	124.3	8.92	55.4	4.61	31.7	2.12, 2.17	36.6	2.36, 2.51				
Q153	123.2	8.81		4.41	29.1	2.03, 2.13	34.0	2.37, 2.43				
V154	122.6	8.37	59.3	4.49	32.5	2.14	20.9	0.99, 0.99				
P155			63.1	4.48	32.1	2.34, 1.94	27.6	2.08, 2.03	50.8	3.91		Hδ′3.73
Q156	120.4	8.51	55.2	4.33		2.12, 2.02		2.43, 2.35				
Q157	122.1	8.44		4.68	28.7	2.14, 2.00		2.43				
P158			63.1	4.54		2.35, 2.02	27.6	2.10	50.3	3.73		Hδ′3.83
T159	118.7	7.85	63.1	4.18, 4.28		4.28		1.23				

[a]Experimental conditions: 90% ^2H_2O/10% ^2H_2O, or 99% ^2H_2O, 20 mM potassium phosphate, 150 mM NaCl, 5 mM DTT-d_{10}, pH 6.3, 28°C.

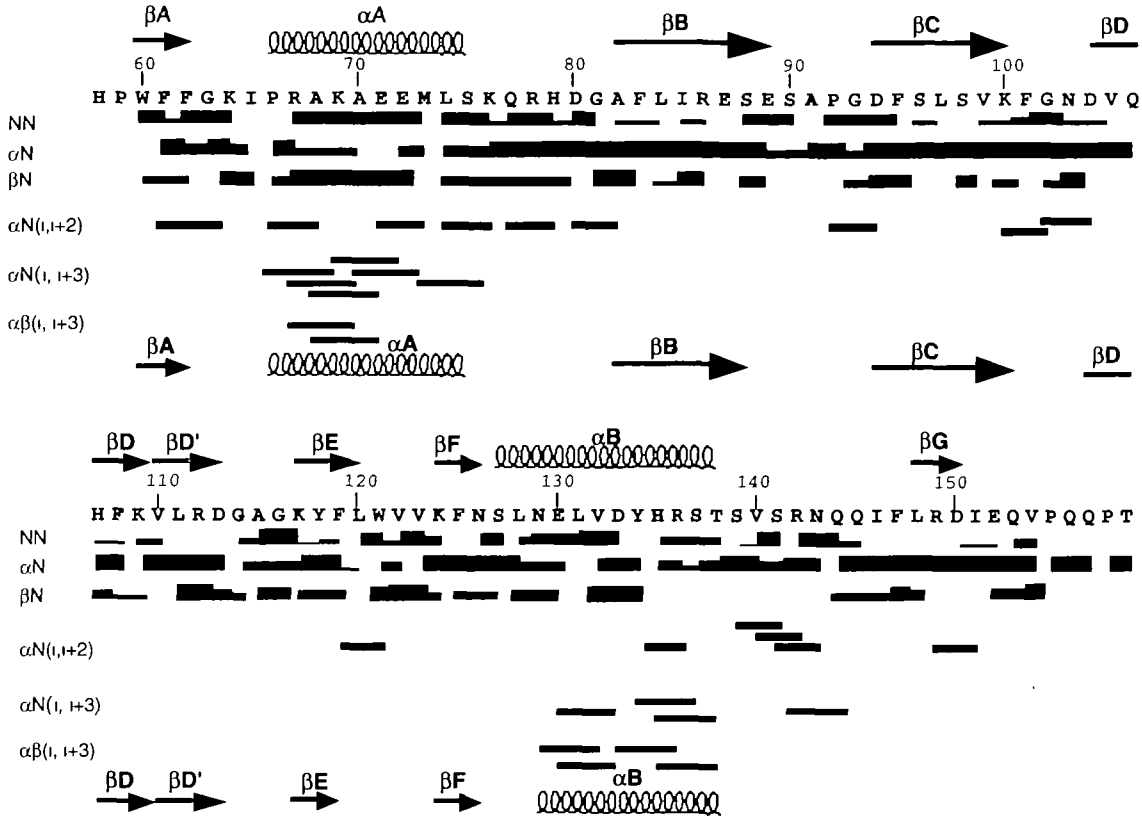

Fig. 3. **Sequential and short-range NOE connectivities of Grb2 SH2 complexed with the EGFR-peptide.** The consensus structural elements of the SH2 secondary structure are shown at the top; the secondary structure as revealed in the present study is shown at the bottom.

129-137. There are also sequential NOE connectivity patterns characteristic of β-strands at residues 60-63 (βA), 82-88 (βB), 94-98 (βC), 103-113 (βD, βD'), 117-119 (βE), and 124-126 (βF). The secondary structure of Grb2/Ash SH2 complexed with the EGFR-peptide from NOE connectivity (at the bottom) was essentially the same as that of the consensus structure shown at the top of Fig. 3. The secondary structure is also consistent with that of the uncomplexed Grb2/Ash SH2 domain (*8*), showing that only minor sturctural changes are induced by the binding of the EGFR-peptide. The secondary structure of the Grb2/Ash SH2 domain was further investigated through NOE correlations between β-strands and the alignment of the β-strands is summarized in Fig. 4. βA and βB form a parallel β-sheet. Extensive NOE correlations were observed between the βB and βC and the βC and βD strands, which form a triple-stranded antiparallel β-sheet structure. βD', βE, and βF form a loosely attached triple stranded antiparallel β-sheet. Except for the absence of the βG strand, the alignment of the secondary structure of Grb2/Ash SH2 complexed with the EGFR-peptide is quite similar to those of other SH2 domains (*11*).

Binding Experiments of EGFR-Peptide—In order to correlate the NMR resonances in the free and complexed forms of Grb2/Ash SH2, aliquots of EGFR-peptide solution were successively added to Grb2/Ash SH2 solution at molar ratios of 0.2, 0.4, 0.6, 0.8, 1.0, 1.2, 1.5, and 2.0. Most resonances shifted gradually, characteristic of a fast exchange process, showing that the binding affinity of the EGFR-peptide to Grb2/Ash SH2 is not strong and k_{off} is faster than the chemical shift time scale. Figure 5, (a) and (b), shows chemical shift changes of the main chain amide proton and nitrogen resonances between the free and complex forms, respectively, in absolute values. Large chemical shift changes of more than 0.25 ppm for the amide protons and 1.0 ppm for the amide nitrogens were observed for residues Phe 61, Ala 68, Ser 88, Glu 89, Gly 93, Phe 95, His 107, Phe 108, Lys 109, Leu 120, Trp 121, Val 122, and Val 123. These residues were mapped on the structure of Grb2/Ash SH2 (Fig. 6). Large chemical shift changes were induced for residues on αA, βA, βB, βC, and βD and the BC and EF loops. However, the residues on the BG loop showed no appreciable chemical shift changes. The three-dimensional structures of SH2 complexed with cognate phosphotyrosine-containing peptides have been determined by X-ray crystallography and NMR spectroscopy (*11*). These studies revealed that phosphotyrosine-containing peptides bind to SH2 at two sites. The first binding site is a conserved pocket lined by consensus basic residues that accommodates the phosphotyrosine residue. The pocket is comprised of residues on βC, βD, αA, and the BC loop. The second binding site is more variable in several SH2 domains and recognizes specific amino acid residue(s) on the C-terminal side of the phosphotyrosine residue. The C-terminal peptide sequence is generally recognized by residues on the BG and EF loops. They bite the C-terminal peptide just like a jaw. The present chemical shift perturbation study supports the phosphotyrosine residue being located in the pocket lined by αA, βC, βD, and BC. However, no appreciable chemical shift changes were

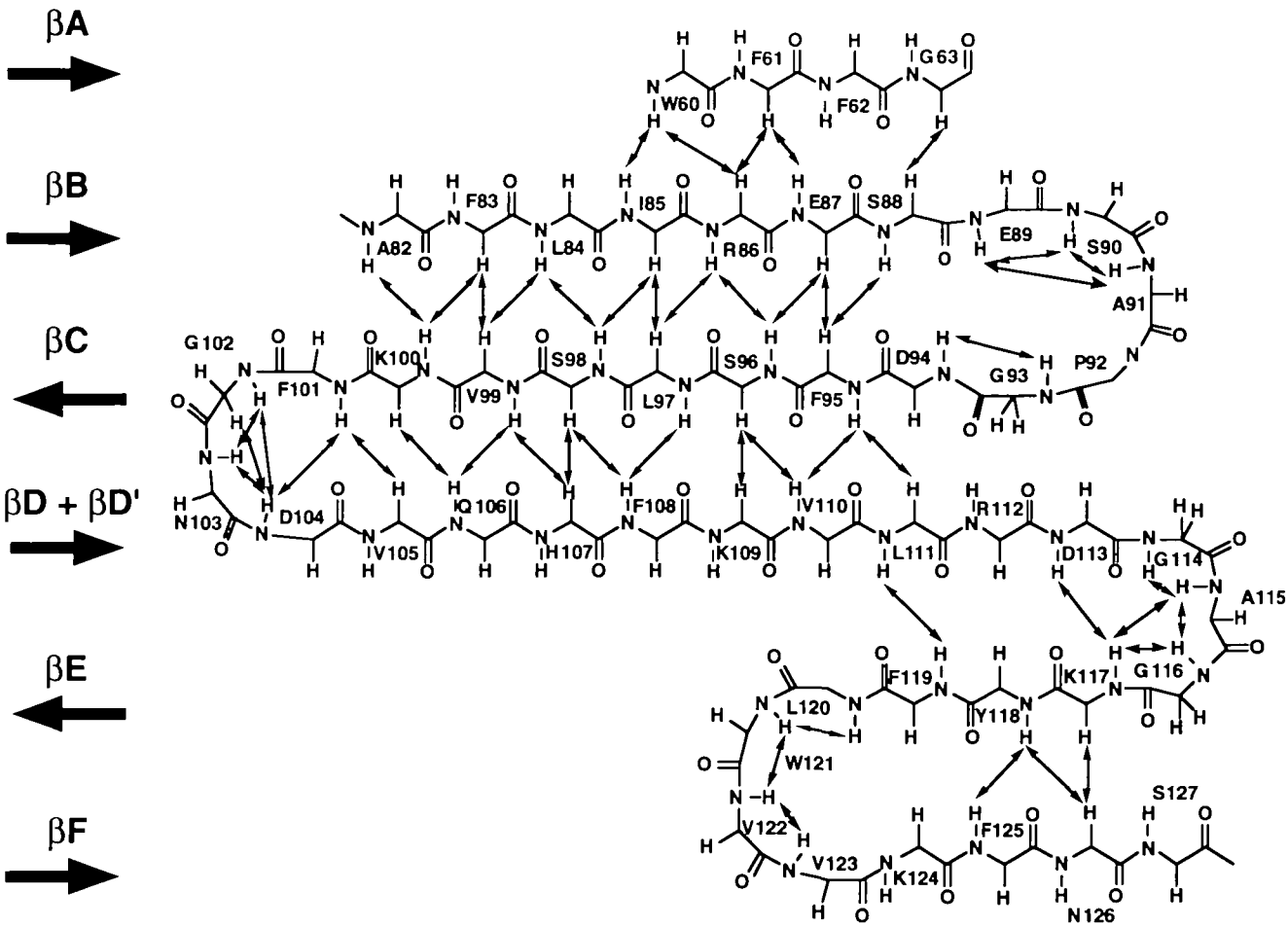

Fig. 4. **Alignment of the β-strands in the Grb2 SH2-EGFR peptide complex.** The NOE connectivities between strands and within the loops are shown by arrows.

observed for the residues on the BG loop, suggesting that Grb2/Ash SH2 recognizes the EGFR-peptide in a different binding mode. Although we tried to determine the conformation of the bound peptide using the filter experiments (*10*), the NMR resonances of the EGFR-peptide are broad in the complex, possibly reflecting an exchange process, so we could not observe intermolecular NOE cross peaks between Grb2/Ash SH2 and the EGFR-peptide.

Fluorescence Measurements of Grb2/Ash SH2 and Its Mutants—We made constructs of several alanine mutants, S141A, R142A, and N143A on the BG loop, and L120A on βE4 of Grb2/Ash SH2, to investigate the contribution of each residue to the binding of the EGFR-peptide. In Fig. 7, we summarize the results of fluorescence measurements with the fluorescence intensities plotted against the concentration of the EGFR-peptide. Analysis of the fluorescence titration curves gave dissociation constant of 2.9 μM for wild type Grb2/Ash SH2. Other mutants gave dissociation constants in the range of 3.2-3.6 μM, similar to that of the wild type. This result, together with the NMR studies of EGFR-peptide binding, suggests that these residues are not involved in EGFR-peptide binding. Recently, the structures of Grb2/Ash SH2 complexed with BCR-Abl- and Shc-derived phosphotyrosine containing peptides were determined by X-ray crystallography (*9*) and NMR spectroscopy (Ogura *et al.*, unpublished results). These studies revealed both peptides to bind to Grb2/Ash SH2 with a turn conformation. Trp 121 blocks the binding of the peptide to form an extended conformation and force the peptide to take a turn conformation. The results of the chemical shift perturbation studies of binding of either Shc or the EGFR-peptide were quite similar, suggesting that both peptides bind to Grb2/Ash in a similar manner. Thus, our results support previous reports that Grb2/Ash SH2 prefers a turn conformation for the bound peptide, unlike the Src family proteins and other SH2 domains. Considering that the downstream signaling from the growth factor receptor is determined by the affinity between the cognate SH2 domain and peptide pair, it is of general interest that SH2 recognizes a specific conformation of the peptide. Grb2/Ash is unique among the known SH2 domains in being the only SH2 domain with a tryptophan residue at EF1 and requiring Asn at pTyr+2 for the binding peptide. Since EF1 is either threonine or glycine in Src or PLC-γ1, the residue at EF1 plays an important role in determining both the conformation and specificity of the binding peptide. Mutation of the threonine residue at position EF1 in Src SH2 to a tryptophan residue has been reported to alter the specificity of Src SH2 to Grb2/Ash-type (*12*). It is the topography of the binding surface of SH2 that is respon-

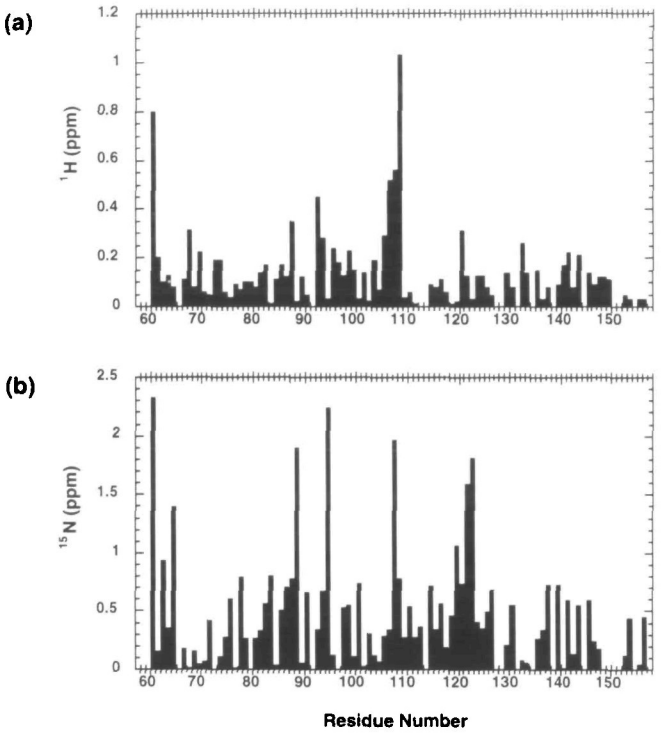

Fig. 5. **Chemical shift changes for each backbone amide group of the Grb2 SH2 domain induced by complex formation with the EGFR-peptide, where the chemical shift changes are presented in absolute values.** Upper and lower panels show backbone (a) ^{1}H and (b) ^{15}N chemical shift changes, respectively.

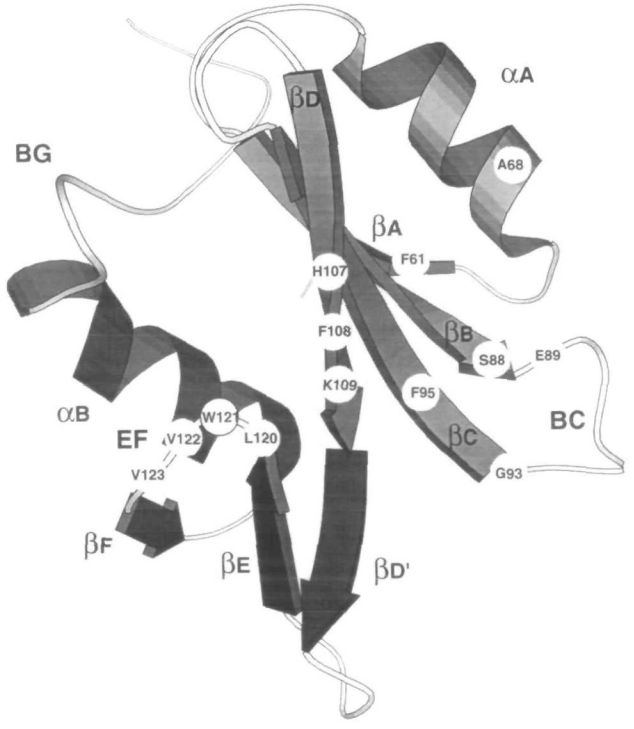

Fig. 6. **Ribbon diagram of the Grb2 SH2 domain complexed with the EGFR-peptide (residues 60-159) (Tsuchiya *et al.*, unpublished results).** Residues whose amide group signals show sizable chemical shift changes upon peptide-binding are mapped on the ribbon diagram.

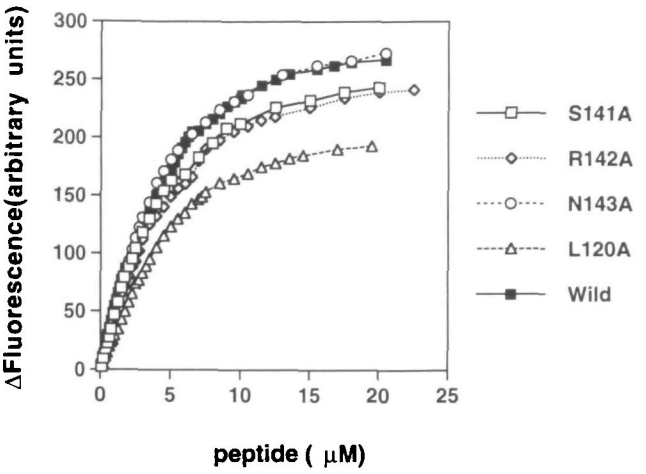

Fig. 7. **The binding affinity of the EGFR-peptide to wild-type and mutant Grb2 SH2.** The fluorescence intensity at 360 nm was measured following the addition of aliquots of the EGFR-peptide. The excitation wavelength was 295 nm with a band width of 5 nm and emission was observed with a band width of 10 nm. ■; wild type; □, S141A; ○, R142A; ◇, N143A; and △, L120A.

sible for determining the specificity of the peptides, and thus determining downstream signaling.

REFERENCES

1. Lowenstein, E.J., Daly, R.J., Batzer, A.G., Li, W., Margolis, B., Lammers, R., Ullrich, A., Skolnik, E.Y., Bar-Sagi, D., and Schlessinger, J. (1992) The SH2 and SH3 domain-containing protein Grb2 links receptor tyrosine kinases to ras signaling. *Cell* **70**, 431-442; Matsuoka, K., Shobata, M., Yamakawa, A., and Takenawa, T. (1992) Cloning of Ash, a ubiquitous protein composed of one Src homology region (SH) 2 and two SH3 domains, from human and rat cDNA libraries. *Proc. Natl. Acad. Sci. USA* **89**, 9015-9019
2. Li, N., Batzer, A., Daly, R., Yajnik, V., Skolnik, E., Chadrin, P., Bar-Sagi, D., Margolis, B., and Schlessinger, J. (1993) Grb2 mediates the EGF-dependent activation of guanine nucleotide exchange on Ras. *Nature* **363**, 83-85
3. Gale, W.N., Kaplan, D., Lowenstein, E.J., Schlessinger, J., and Bar-Sagi, D. (1993) Guanine-nucleotide-releasing factor hSos binds to Grb2 and links receptor tyrosine kinase to Ras signaling. *Nature* **363**, 88-92
4. Buday, L. and Downward, J. (1993) Epidermal growth factor regulates p21ras through the formation of a complex of receptor, Grb2 adapter protein, and Sos nucleotide exchange factor. *Cell* **73**, 611-620
5. Rozakis-Adcock, M., McGlade, J., Mbamalu, G., Pelicci, G., Daly, R., Li, W., Batzer, A., Thomas, S., Brugge, J., Pelicci, P.G., Schlessinger, J., and Pawson, T. (1992) Association of the Shc and Grb2/Sem5 SH2-containing proteins is implicated in activation of the Ras pathway by tyrosine kinases. *Nature* **360**, 689-692
6. Schlaepfer, D.D., Hanks, S.K., Hunter, T., and van der Geer, P. (1994) Integrin-mediated signal transduction linked to Ras pathway by Grb2 binding to focal adhesion kinase. *Nature* **372**, 786-791
7. Songyang, Z., Shoelson, S.E., McGlade, J., Olivier, P., Pawson, T., Bustelo, X.R., Barbacid, M., Hanafusa, H., Yi, T., Ren, R., Baltimore, D., Ratnofsky, S., Feldman, R.A., and Cantley, L.C. (1994) Specific motifs recognized by the SH2 domains of Csk, 3BP2, fes/fps, Grb-2, HCP, SHC, Syk and Vav. *Mol. Cell. Biol.* **14**, 2777-2785
8. Thornton, K.H., Mueller, W.T., McConnell, P., Zhu, G., Saltiel,

A.R., and Thanabal, V. (1996) Nuclear magnetic resonance solution structure of the growth factor receptor-bound protein 2 Src homology 2 domain. *Biochemistry* **35**, 11852-11864
9. Rahuel, J., Gay, B., Erdmann, D., Strauss, A., García-Echeverría, C., Furet, P., Caravatti, G., Fretz, H., Schoepfer, J., and Grütter, M.G. (1996) Structural basis for specificity of Grb2-SH2 revealed by a novel ligand binding mode. *Nature Struct. Biol.* **3**, 586-589
10. Ogura, K., Terasawa, H., and Inagaki, F. (1996) An improved double-tuned and isotope-filtered pulse scheme based on a pulsed field gradient and a wide-band inversion shaped pulse. *J. Biomol. NMR* **8**, 492-498
11. Kuriyan, J. and Cowburn, D. (1997) Modular peptide recognition domains in eukaryotic signaling. *Annu. Rev. Biophys. Biomol. Struct.* **26**, 259-288
12. Marengere, L.E.M., Songyang, Z., Gish, G.D., Schaller, M.D., Parsons, J.T., Stern, M.J., Cantley, L.C., and Pawson, T. (1994) SH2 domain specificity and activity modified by a single residue. *Nature* **369**, 502-505
13. Bax, A. and Subramanian, S. (1986) Sensitivity-enhanced two-dimensional heteronuclear shift correlation NMR spectroscopy. *J. Magn. Reson.* **67**, 565-569
14. Marion, D., Driscol, P.C., Kay, L.E., Wingfield, P.T., Bax, A., Gronenborn, A.M., and Clore, G.M. (1989) Overcoming the overlap problem in the assignment of ^{1}H NMR spectra of larger proteins by use of three-dimensional heteronuclear ^{1}H-^{15}N Hartmann-Hahn-multiple quantum coherence spectroscopy: application to interleukin 1b. *Biochemistry* **28**, 6150-6156
15. Delaglio, F., Grzesiek, S., Vuister, G.W., Zhu, G., Pfeifer, J., and Bax, A. (1995) NMR Pipe: A multidimensional spectral processing system based on UNIX pipes. *J. Biomol. NMR* **6**, 277-293
16. Hatanaka, H., Oka, M., Kohda, D., Tate, S., Suda, A., Tamiya, N., and Inagaki, F. (1994) Tertiary structure of erabutoxin b in aqueous solution as elucidated by two-dimensional nuclear magnetic resonance. *J. Mol. Biol.* **240**, 155-166
17. Cavanagh, J., Fairbrother, W.J., Palmer III, A.G., and Skelton, N.J. (1996) *Protein NMR Spectroscopy, Principles and Practice*, Academic Press, New York
18. Grzesiek, S., Anglister, J., and Bax, A. (1993) Correlation of backbone amide and aliphatic side-chain resonances in ^{13}C/^{15}N-enriched proteins by isotropic mixing of ^{13}C magnetization. *J. Magn. Reson.* **B101**, 114-119
19. Clubb, R.T., Thanabal, V., and Wagner, G. (1992) A new 3D HN(CA)HA experiment for obtaining fingerprint H^N-H^α cross peaks in ^{15}N- and ^{13}C-labeled proteins. *J. Biomol. NMR* **2**, 203-210
20. Seip, S., Balbach, J., and Kessler, H. (1992) An Improved technique for correlating backbone amide protons with ^{15}N and H^α protons (HN(CA)H) in isotopically enriched proteins. *J. Magn. Reson.* **100**, 406-410